Assessing sound absorption coefficient under a synthesized diffuse acoustic field: effect of the sample size and nature

Olivier Robin[a]
Celse Kafui Amedin[b]
Alain Berry[c]
Noureddine Atalla[d]
Groupe d'Acoustique de l'Université de Sherbrooke - 2500, Boulevard de l'Université
Sherbrooke (Québec) J1K2R1 - Canada

Olivier Doutres[e]
École de Technologie Supérieure 1100, rue Notre-Dame Ouest
Montréal (Québec) H3C1K3 - Canada

Franck Sgard[f]
Institut de Recherche en Santé et Sécurité du Travail 505, boul. De Maisonneuve Ouest
Montréal (Québec) H3A3C2 - Canada

A method for estimating the sound absorption coefficient of a material under a synthesized Diffuse Acoustic Field was recently proposed, as an alternative to classical sound absorption measurements in reverberant rooms. Using sound field reproduction approaches and a synthetic array of acoustic monopoles facing the material, estimation of the sound absorption coefficient under a reproduced Diffuse Acoustic Field but in free-field conditions was shown to be feasible. The method was successfully tested on two samples of melamine foam of close thicknesses and areas.

In this paper, the principle of the method will be first recalled. The effect of varying the reproduction array size on the calculated sound absorption coefficients is then studied. A comparative measurement between the suggested method and the reverberant room method on ceiling tiles is finally reported.

[a] Email: olivier.robin@usherbrooke.ca
[b] Email: celse.kafui.amedin@usherbrooke.ca
[c] Email: alain.berry@usherbrooke.ca
[d] Email: noureddine.atalla@usherbrooke.ca
[e] Email: olivier.doutres@etsmtl.ca
[f] Email: franck.sgard@irsst.qc.ca

1 INTRODUCTION

The sound absorption coefficient of absorbing materials under a Diffuse Acoustic Field (DAF) excitation is classically measured using the normalized Reverberant Room method, described in ISO 354[1] and ASTM C423[2]. Both standards provide several recommendations in order to increase measurement accuracy, such as verifying that either minimum reverberation time or sufficient sound field homogeneity are ensured (as examples, a maximum equivalent absorption area for ISO354, or a maximum decay rate standard deviation between different receivers for ASTM C423).

In order to meet the standards specifications (i.e. usually improving room's diffusivity), various types of diffusers (hanging, rotating, corner or boundary) are commonly used, but for years their optimal number or type has been a debated subject[3-6] as well as the indicators used to properly qualify the sound field diffusivity[6,7]. Size, distribution, position and nature effects of tested materials are also of great importance on the results obtained[8-10], with values of absorption coefficients that can exceed unity (and then rounded to unity or less to perform room acoustic simulations as an example). As a general consequence and despite the standards requirements, a poor inter-laboratory reproducibility of measured absorption coefficients under DAF excitation was reported in several recent[11,12] and former[13,14] studies, even when testing the same specimen. The reverberant room is used as a laboratory tool to recreate an experimental excitation as close as possible to its mathematical model[15], but the limitations cited above might then be encountered.

This paper proposes an alternative approach for the estimation in free-field conditions of the absorption coefficient of an absorbing material under a synthesized DAF excitation at the material surface by using a synthetic array of acoustic monopoles facing the material. The method consists of two steps: (1) a database of measured reflection coefficients at normal and oblique incidence angles is first generated with the classical two-microphone approach and a source-image model, using a point source that is moved over a plane parallel to the material surface, and (2) sound field reproduction approaches are then used to calculate a Cross-Spectral Density (CSD) matrix of source amplitudes to accurately reproduce the theoretical statistical properties of a DAF excitation on the material surface using the synthetic array. Coupling this calculated matrix to the measured reflection coefficients database, allows estimating in a post processing phase the absorption coefficient under a synthetic DAF.

The method was validated on samples of melamine foam of comparable thicknesses and areas[16]. This paper first recalls the principles of the method. Some insights are then provided about the array size effects using additional post-processing of the database used for the validation cases. Additional experimental results on tiles are finally provided. Results of numerical simulations that are currently underway will be shown and discussed during the oral presentation.

2 THEORY

2.1 Sound absorption coefficient under a single point source

Figure 1(a) describes a simple and well-known situation[17]. A single point source is positioned at a given position i at a height $z=z_s$ above a layer of porous material. Two microphones denoted M_1 and M_2 are placed above the porous material and centered on its surface at heights $z=z_1$ and $z=z_2$, respectively. Under the assumption of an ideal point source (defined by its volume acceleration $q_i(\omega)$), the acoustic field at any of the microphone positions is a superposition of

two spherical acoustic waves, generated by the source q_i (ω) and the corresponding image source q'_i (ω) positioned at a distance r_i and a distance r'_i from the receiver, respectively. For a small separation of the two microphones so that the angle θ_i is almost identical for both microphones, the measured acoustic pressure $p_{ij}(\theta_i,\omega)$ for a given position i of the point source at microphone M_j (j=1,2) can be written[17]

$$p_{ij}(\theta_i,\omega) = \rho_0 q_i(\omega)\frac{e^{-jk_0 r_{ij}}}{r_{ij}} + R(\theta_i,\omega)\rho_0 q'_i(\omega)\frac{e^{-jk_0 r'_{ij}}}{r'_{ij}}, \qquad (1)$$

with ρ_0 the air mass density, ω the angular frequency, k_0 the acoustic wavenumber (k_0=ω/c_0) with c_0 the speed of sound), r_{ij} the distance between the source at the i-th position and the microphone M_j, r'_{ij} the distance between the image source and the microphone M_j and $R(\theta_i,\omega)$ is the reflection coefficient of the material surface corresponding to the i-th position of the point source. The measurement of $H(\theta_i,\omega)$=$p_{i2}(\theta_i,\omega)$ / $p_{i1}(\theta_i,\omega)$ allows for calculating the reflection coefficient at a given incidence angle using the classical relation[17]

$$R(\theta_i,\omega) = \frac{\frac{e^{-jk_0 r_{i2}}}{r_{i2}} - H(\theta_i,\omega)\frac{e^{-jk_0 r_{i1}}}{r_{i1}}}{H(\theta_i,\omega)\frac{e^{-jk_0 r'_{i1}}}{r'_{i1}} - \frac{e^{-jk_0 r'_{i2}}}{r'_{i2}}}. \qquad (2)$$

The corresponding absorption coefficient can be deduced using the relation $\alpha(\theta_i,\omega)$=1 - $|R(\theta_i,\omega)|^2$.

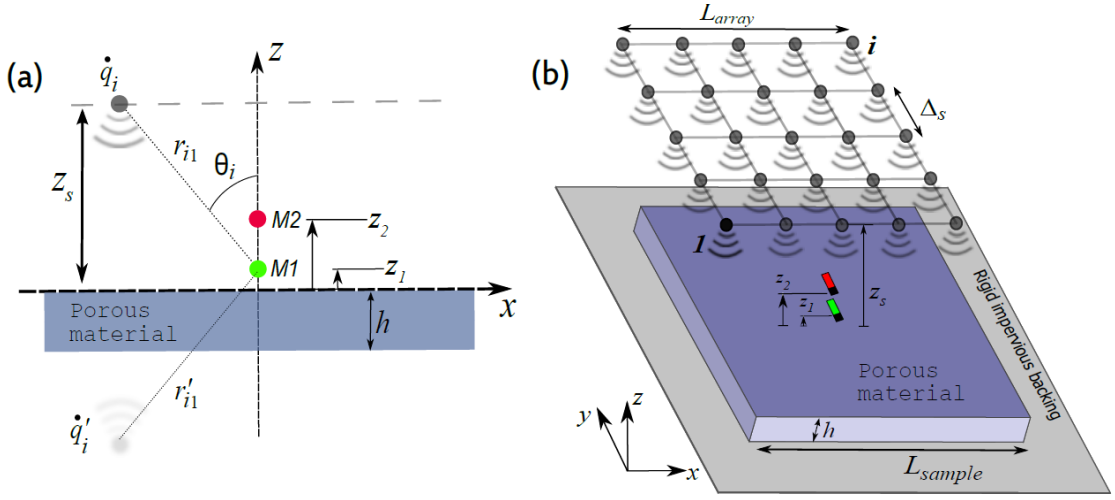

*Fig. 1 – (a) Description of the problem and coordinate system for a spherical wave model using a single point source – (b) Description of the problem using an **i**-source array, with uniformly distributed sources positioned with the same source separation Δ_s [adapted from Robin et al.[16]].*

2.2 Sound reflection coefficient under a synthesized pressure field

Figure 1(b) illustrates the proposed approach. A square sample of porous material of sidelength L and thickness h is placed on a rigid impervious backing. The two microphones *M1* and *M2* and the array center point source are centered on the material's surface. Using the two-microphones method described in the previous section, the reflection coefficient can be measured under various incidence angles corresponding to successive source positions i of point sources, thus creating a virtual array of monopoles in front of the material surface. The Green's

functions corresponding to the propagation from the real (respectively image) point source to the microphone M_j will now be denoted $g_{ij}(\omega) = e^{-jk_0 r_{ij}}/r_{ij}$ (respectively $g'_{ij}(\omega) = e^{-jk_0 r'_{ij}}/r'_{ij}$).

It can be shown (calculation details can be found in Robin[16]) that with a database of measured reflection coefficients $R(\theta_i,\omega)$ at several i incidence angles and a calculated CSD matrix of source volume accelerations $\boldsymbol{S_{QQ}}$ (that when applied to all the virtual sources would lead to the reproduction of a desired pressure field at the material surface), Eq. (3) below provides the squared reflection coefficient $|R_{synth}(\omega)|^2$ under a synthesized pressure field at a post-processing phase

$$\left|R_{synth}(\omega)\right|^2 = \frac{\boldsymbol{h_1^H S_{QQ} h_1}}{\boldsymbol{g_1'^H S_{QQ} g_1'}}, \tag{3}$$

where $\boldsymbol{h_1} = \{\cdots\ g_{i1}(\omega)\cdots\}^T, \boldsymbol{g'_1} = \{\cdots\ R(\theta_i,\omega)g'_{i1}(\omega)\cdots\}^T$ and ^{T} denotes the non-conjugate transpose. Note that the two microphones are needed for the calculation of the individual reflection coefficients $R(\theta_i,\omega)$ (following the procedure described in previous section), but the calculation of the squared reflection coefficient under a synthetic pressure field $|R_{synth}(\omega)|^2$ is finally made for only one microphone position.

The corresponding absorption coefficient can be deduced using the relation $\alpha_{synth}(\omega) = 1 - |R_{synth}(\omega)|^2$. Note here that the squared absolute reflection coefficient used for this calculation is calculated at a specific position on the material surface (contrary to the 'global' absorption result directly obtained with the reverberant room method as an example), and could then be used to deduce a mean absorption value with measurements made along the material surface, or even plotting absorption maps. The CSD matrix of source volume acceleration $\boldsymbol{S_{QQ}}$ can be calculated using either a Wave Field Synthesis (WFS) approach[18] or a Planar Nearfield Acoustical Holography (P-NAH) approach[19] (in this paper, the latter is always used), with a target pressure field defined by the CSD of a DAF[15].

2.3 Measurement and simulation results

Reverberant room absorption tests of melamine foam of 0.0762 m (3 inches) thickness and 5.94 m^2 area were made in the National Research Canada (NRC) reverberant room (volume ≈ 258 m^3) following ASTM C423[2]. A sample of the same material of 2.11 m^2 was tested following the proposed approach in an anechoic room. The sample was laid on a rigid impervious backing, made up from a 1/2 inch thick medium density fiberboard panel covered with a 1/32 inch steel plate. An omnidirectional point source was manually translated using a rigid frame on a mesh of 7 by 7 positions above the material surface at a height z_s=0.2 m, with the center source position corresponding to the normal incidence case (i.e. the two microphones are placed at the vertical of this source position). The source separation Δ_s was set to 0.15 m with a corresponding virtual array sidelength L_{array} of 0.9 m. The maximum incidence angle θ_{max} that can be included in the database of measured reflection coefficients is defined by the separation z_s between the source and the material surface (the reproduction plane) and the largest source to microphones distance. In the present case, $\theta_{max}=\tan^{-1}(L_{array}/\sqrt{2}.z_s) \approx 72°$.

On the other hand, simulations based on the Transfer Matrix Method (TMM)[20] were performed. The layer of homogeneous material of infinite extent and backed by a hard wall was modeled under a limp frame assumption[20]. The parameters given in table 1 were used in simulations to compute the characteristic impedance Z_{ceq} and the wavenumber k_{eq} of the equivalent fluid element *via* the Johnson-Champoux-Allard model. Since the DAF theoretically reproduced with

the synthetic array implies a maximum incidence angle of 72°, the same maximum incidence value was used as an upper bound to define the DAF excitation in the numerical simulations.

Table 1 – Measured parameters for the tested melamine foam

Parameter	Tortuosity α_∞ [-]	Porosity Φ [-]	Resistivity σ [Nm^{-4}s]	Viscous length Λ [μm]	Thermal length Λ' [μm]	Foam mass density ρ_1 [kg.m^{-3}]
Value	1	0.99	10900	100	130	8.8

The results obtained are reported in Fig. 2 (for further details or additional results, please refer to [16]). Above the 500 Hz third octave band, the estimated absorption coefficients using a synthesized DAF excitation are in good agreement with those obtained by simulations for an infinite material, with a difference below 0.1. Furthermore, results are within a physical range (i.e., between 0 and 1), and do not exhibit size effects as seen in reverberant room results even if smaller samples were used. The differences seen below 500 Hz are mainly thought to be related to the finite side length of the array, but the finite size of the sample may also explain these low frequency limitations and discrepancies with TMM results (since this simulation assumes laterally infinite material). The effect of the finite side length of the array is studied in the next section.

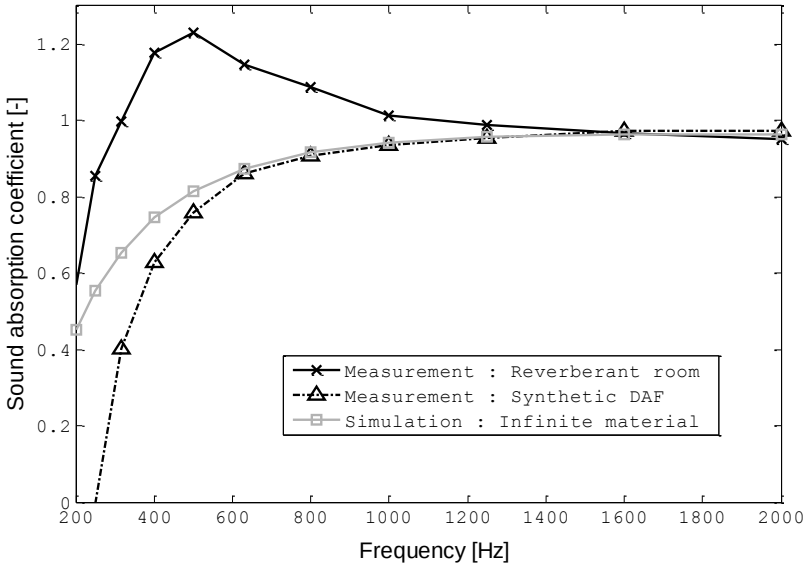

Fig. 2 – Measurement and simulation results for a 3-inch thick melamine foam.

3 EFFECT OF ARRAY SIZE ON THE CALCULATED ABSORPTION COEFFICIENT

In order to better understand the possible array size effects, additional post-processing were made using two databases obtained on the previously presented melamine foam, and on another sample of the same material of 2 inches thickness and 1.69 m^2 area. For both samples, a database of 49 measured reflection coefficients (corresponding to 7x7 source positions) was previously built using similar source separation Δ_s and source height z_s.

Using this database, the size of the virtual array is then varied at the post-processing while keeping the same target pressure to be reproduced (i.e. a theoretical DAF with angles of incidence up to 90°). Figure 3 illustrates the corresponding geometries.

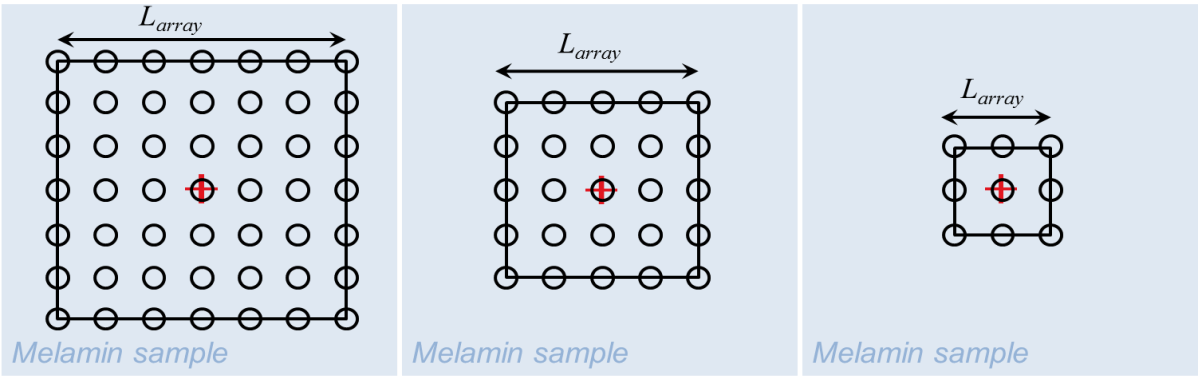

Figure 3 – (a) Original measurement mesh (7x7), (b) Reduced measurement mesh (5x5), (c) Reduced measurement mesh (3x3) – The position of the vertical microphone doublet is indicated by a red cross.

Sound absorption coefficients under a synthesized DAF are then calculated following the procedure described in Section 2.2 with arrays of 3x3, 5x5 and 7x7 sources (i.e. L_{array}=0.3 m, 0.6 m and 0.9 m, respectively, with a fixed size of the material sample). This dimension theoretically puts a limit to the larger wavelength (or lower frequency) that could be reproduced, which is simply the wavelength corresponding to L_{array}. With the speed of sound c_0 taken equal to 345 m/s, the corresponding lowest frequencies ($=c_0/L_{array}$) for the 3x3, 5x5 and 7x7 cases are 1150 Hz, 575 Hz and 383 Hz, respectively. By doing this, the side length of the array is reduced, but the same also applies to the highest incidence angle included in the reflection coefficients database, the two microphones being located at the vertical of the center source. The maximum incidence angle θ_{max} is approximately 72° in the case of the 7x7 sources configuration (and $\theta max \approx 64°$ for the 5x5 configuration and $\theta_{max} \approx 46°$ for the 3x3 configuration). The corresponding TMM simulations were made using the same highest incidence angles.

The results obtained are given in Figures 4(a-f) for thicknesses of 3 inches and 2 inches, respectively. When the array size is increased, the agreement between the results obtained using the proposed method and simulations is always very satisfactory above the third octave frequency band that nearly corresponds to the lowest frequency that could be reproduced (that is above the 1000 Hz third octave band for the 3x3 sources case, above the 630Hz third octave band for the 5x5 case and above the 400 Hz third octave band for the 7x7 case). This effect is especially noticeable in the 2-inch melamine foam case (Figs. 4(d-f)) and was found to be lower in the case of the highly absorbing 3 inches melamine foam (Fig. 4(a-c)), but this was not explained. Note that the TMM simulations provide very similar results for the 3 inches thickness, indicating that the incidence angle effect is theoretically lower when the thickness is increased. Below the 400 Hz third octave band, the accuracy of the method seems insufficient for both thicknesses, with absorption coefficients that either decrease quickly to zero and even negative values for the 3-inch melamine case (Fig. 4(c)) or remain nearly constant for the 2-inch melamine case (Fig. 4(f)). This is mainly attributed to a finite size effect of the array.

Interestingly, these results suggest that using a database including a given highest incidence angle, the absorption coefficient under a DAF excitation with other (i.e. equal or lower) incidence angles could be then computed at the post-processing step (however limited by the low frequency bound defined by the corresponding size of the array). Also, a larger array size could give the possibility of measuring the absorption coefficient for incidence angles higher than the field incidence angle (i.e. 78°) usually considered to perform representative simulations of measurements made in a reverberant room.

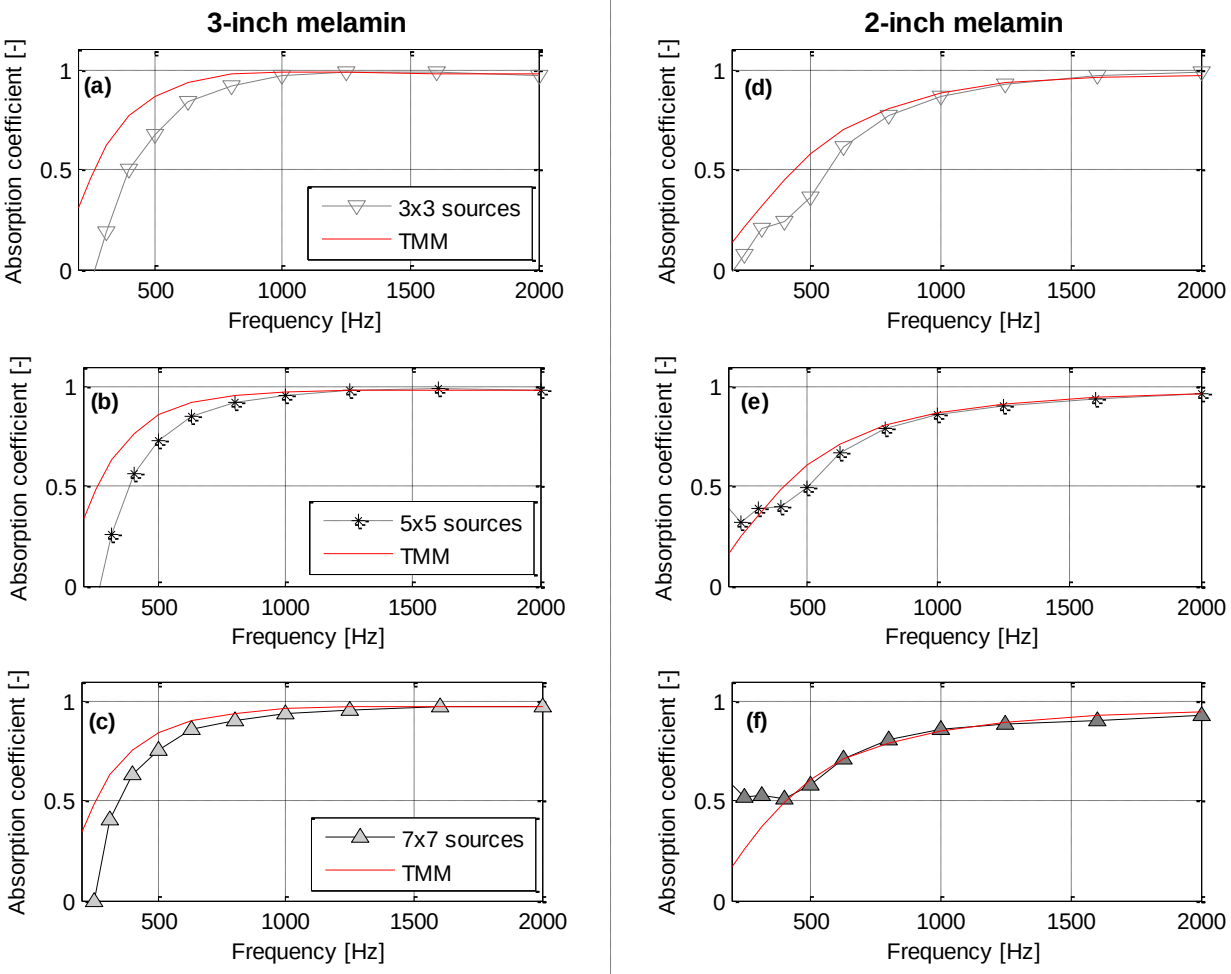

Figure 4 – 3-inch melamine case: results obtained for (a) a 3x3 array and a simulation $\theta_{max}=46^o$, (b) a 5x5 array and a simulation using $\theta_{max}=64^o$, (c) a 7x7 array and a simulation using $\theta_{max}=72^o$-- 2-inch melamine case: results obtained for (d) a 3x3 array and a simulation using $\theta_{max}=46^o$, (e) a 5x5 array and a simulation using $\theta_{max}=64^o$, (f) a 7x7 array and a simulation using $\theta_{max}=72^o$

4 MEASUREMENTS ON CEILING TILES

Finally, to evaluate the possible range of applications for the approach, measurements were conducted on a typical ceiling tile, using the reverberant room method and the proposed method. Each tile was 0.5 m by 0.5m, with small bevels on all four edges for mounting and tile-to-tile assembly (see Figs. 5(a,b)). Their surface was impervious and rigid, and the small back cavity was filled with a felt pad provided with each tile (see Fig. 5(b)).

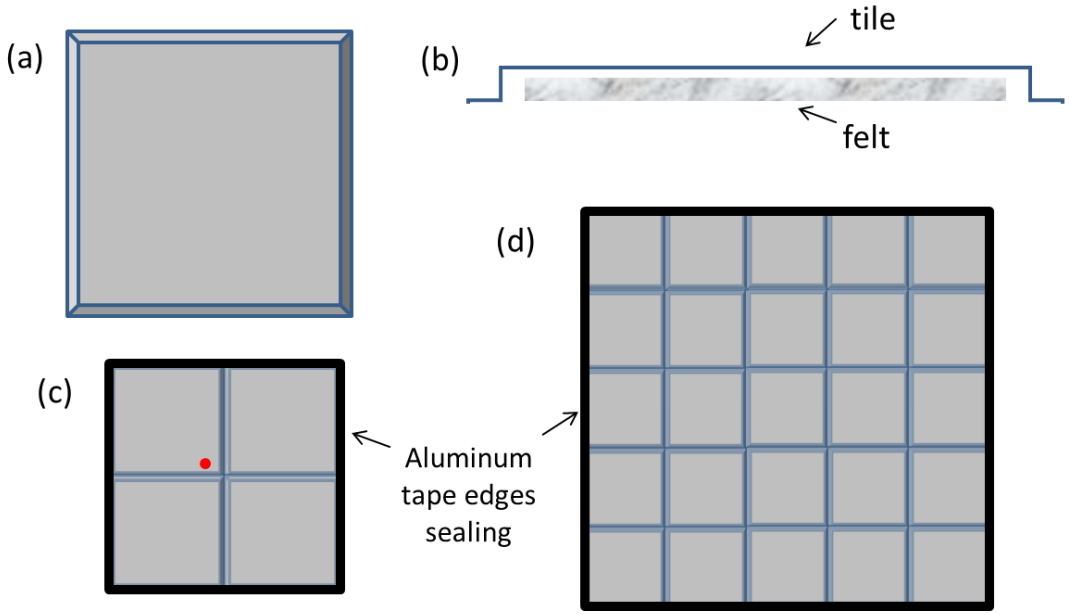

Figure 5 – Sketches of the tiles tested using the reverberant room method and the proposed approach, not to scale (a) Front view of a single tile – (b) Sideview of a single tile – (c) Position of the center point source (and fixed microphones) above the four tiles arrangement tested using the proposed approach – (d) 25 tiles arrangement for the reverberant room measurement.

Concerning the reverberant room measurement, a set of 25 tiles was laid directly on the room floor, and the perimeter of the 25 tiles arrangement was sealed using aluminum tape. The measurement was made following ASTM C423[2] in the Groupe d'Acoustique de l'Université de Sherbrooke reverberant room (volume ≈ 143m^3).
Concerning the proposed method, a set of 4 tiles was implemented with identical conditions than those described in section 2.3 (i.e. laid on a rigid impervious backing in an anechoic room, and a 7 x 7 sources array with source separation Δ_s=0.15 m and source height z_s=0.2 m). The two microphones were positioned slightly offset with respect to the middle of the four tiles arrangement (see Figure 5(c)), to avoid being placed just above the junction area of the tiles.

Figure 6 reports the obtained results. The measurement results with the reverberant room method exhibits a peak of absorption at the 500 Hz third octave band, which is attributed to the mechanical resonance of the tile's frame (together with the spring constituted by the small air gap filled by the porous material). Below this peak, the measured absorption quickly decreases to a value of 0.1 at the 200 Hz third octave banc, while it slowly decreases above this peak to a value of 0.3 at the 2000 Hz third octave band.

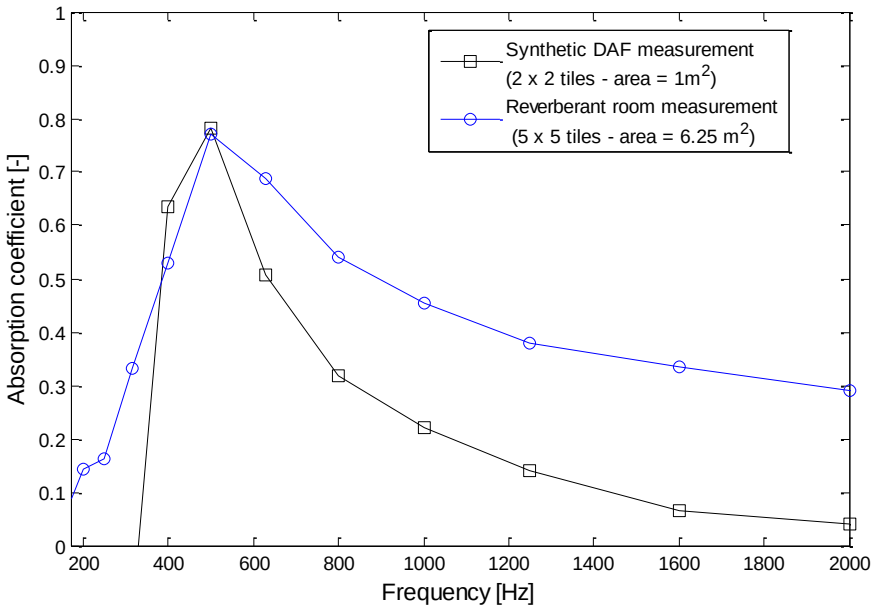

Figure 6 – Measurement results on tiles.

As for the cases reported in section 3, the measured absorption coefficients with the presented method quickly decreases to non-physical values below the 400 Hz third octave band. The absorption peak value is very well captured, with a difference of 0.1 between the two methods. Above this peak, the measured absorption values with the presented approach are systematically below those obtained with the reverberant room method (but interestingly, the method seems able to estimate small absorption values in this frequency range). This difference of absorption values above the peak is mainly attributed to two facts:

(1) the absorption coefficient is locally estimated for the proposed approach (and close to a junction point),

(2) the larger tile arrangement in the reverberant room corresponds to a higher equivalent sound absorption area, and above all, the fact that only the perimeter was sealed also allows higher acoustic leaks around the numerous unsealed edges (see Fig.5(d)) and higher absorbing effect of the felt layers.

Note finally that the global trend obtained with the proposed method is comparable to the one obtained with the reverberant room, with a sample surface reduced by a 6.25 factor.

6 CONCLUSIONS

A method for the estimation in free-field conditions of the absorption coefficient of an absorbing material under a synthesized DAF excitation was presented. The theory concerning the estimation of absorption coefficient under synthesized pressure fields was briefly described. A typical experimental result previously obtained was given, that showed that the estimated absorption coefficients using a synthesized DAF excitation were in good agreement with those obtained from the TMM for homogeneous materials above the 400 Hz third octave band, within a physical range and did not exhibit size effects as seen in reverberant room results.

The effect of varying the source array size on the calculated absorption coefficients was then illustrated on two melamine foam samples of comparable thickness and area. The method was

finally applied to tiles, and the results obtained with the standard reverberant room and the presented method compare reasonably well, even if the sample area was greatly reduced.
Further work is needed to fully understand the strengths and limitations of the method, especially in the low-frequency domain, and this is currently underway using numerical simulations of the method.

7 ACKNOWLEDGEMENTS

This research was supported by Institut de Recherche en Santé et Sécurité du Travail (IRSST).

8 REFERENCES

1. ISO 354:2003, *Acoustics -- Measurement of sound absorption in a reverberation room*, International Standard Organization, Geneva, Switzerland, (2003).

2. ASTM Standard C423-09a, *Standard Test Method for Sound Absorption and Sound Absorption Coefficients by the Reverberation Room Method*, ASTM International, West Conshohocken, PA (2009).

3. C.E. Ebbing, "Experimental evaluation of moving sound diffusers for reverberant rooms," *J. Sound Vib.* **16**(1), 99-108 (1971).

4. K. Bodlund, "A study of diffusion in reverberation chambers provided with special devices," *J. Sound Vib.* **50**(2), 253-283 (1977)

5. D.T. Bradley, C. Diaz and E. Snow, "Improved sound field reverberance and diffusivity in a reverberation chamber though implementation of resonant-diffusing wall panels," *Acta Acust. United Ac.* **101**, 181-189 (2015).

6. D.T. Bradley, M. Müller-Trapet, J. Adelgren and M. Vorländer, "Effect of boundary diffusers in a reverberation chamber: Standardized diffuse field quantifiers," *J. Acoust. Soc. Am.* **135**(4), 1898-1906 (2014).

7. T.J. Schultz, "Diffusion in reverberation rooms, *J.Sound Vib.* 16(1), 17-28 (1971), Pages,

8. J. Parkinson, "Area and pattern effects in the measurement of sound absorption," *J. Acoust. Soc. Am.* **2**(1), 112-122 (1930).

9. V.L. Chrisler, "Dependence of sound absorption upon the area and distribution of the absorbent material," *J. Res. Natl. Bur. Stand.*, **13**(2), 169-187, Research paper RP700 (1934).

10. A. Cops, J. Vanhaecht and K. Leppens, "Sound absorption in a reverberation room: Causes of discrepancies on measurement results," *Applied Acoustics* **46**, 215-232 (1995).

11. N.-A. Andersson, "Sound absorption Round Robin test," In *Proceedings of Forum Acusticum 2011*, 27 June – 01 July, Aalborg, Denmark (2011).

12. A. Nash, “On the reproducibility of measuring random incidence sound absorption,” In *Proceedings of Internoise 2012*, 19-22 August, New-York City, USA, 1-12 (2012).

13. C.W. Kosten, “International comparison measurements in the reverberation room,” *Acustica* **10**, 400-411 (1960).

14. R.E. Halliwell, “Inter-laboratory variability of sound absorption measurement,” *J. Acoust. Soc. Am.* **73**(3), 880-886 (1983).

15. B. Rafaely, “Spatial-temporal correlation of a diffuse sound field,” *J. Acoust. Soc. Am.* **107**, 3254–-3258 (2000).

16. O. Robin, A. Berry, O. Doutres and N. Atalla, “Measurement of the absorption coefficient of sound absorbing materials under a synthesized diffuse acoustic field,” *J. Acoust. Soc. Am.* 136 (1), EL13-19 (2014).

17. J.F. Allard and Y. Champoux, “In-situ two-microphone technique for the measurement of the acoustic surface impedance,” *Noise Control Engineering Journal*, **32**(1), 15–23 (1988).

18. A. Berry, R. Dia and O. Robin, “A Wave Field Synthesis approach to reproduction of spatially-correlated sound fields,” *J. Acoust. Soc. Am.* **131**(2), 1226–1239 (2012).

19. O. Robin, A. Berry and S. Moreau , “Reproduction of random pressure fields based on planar nearfield acoustic holography,” *J. Acoust. Soc. Am.* **133**(6), 3885–3899 (2013).

20. J.-F. Allard and N. Atalla, *Propagation of Sound in Porous Media: Modelling Sound Absorbing Materials*, 2nd edition (Wiley, Chichester, UK, 2009).